Available online at www.sciencedirect.com
SCIENCE DIRECT
Biochemical Pharmacology 68 (2004) 1797–1805
Biochemical Pharmacology
www.elsevier.com/locate/biochempharm

Membrane permeation characteristics of abacavir in human erythrocytes and human T-lymphoblastoid CD4$^+$ CEM cells: comparison with (−)-carbovir

William B. Mahony[a,b], Barbara A. Domin[a,b], Susan M. Daluge[a,*], Thomas P. Zimmerman[b]

[a]*Division of Medicinal Chemistry, GlaxoSmithKline, Research Triangle Park, NC 27709, USA*
[b]*Bayer HealthCare LLC, Biological Products Division, P.O. Box 507, Clayton, NC 27520, USA*

Received 22 April 2004; accepted 25 June 2004

Abstract

Abacavir, (−)-(1*S*,4*R*)-4-[2-amino-6-(cyclopropylamino)-9*H*-purin-9-yl]-2-cyclopentene-1-methanol, is a novel purine carbocyclic nucleoside analogue that has been approved by the FDA for the treatment of HIV (as Ziagen™ [abacavir sulfate]). Chemically, abacavir and (−)-carbovir (CBV) differ only at the 6-position of the purine ring; abacavir contains a cyclopropylamino moiety in place of the 6-lactam functionality of CBV. Intracellularly both are ultimately metabolized to CBV triphosphate. We compared the membrane permeation characteristics of these two compounds at 20 °C in human erythrocytes and in human T-lymphoblastoid CD4$^+$ CEM cells, using a ''papaverine-stop'' assay. In erythrocytes, abacavir influx was rapid, nonsaturable (rate constant = 200 pmol/s/mM/μl cell water), and unaffected by inhibitors of nucleoside or nucleobase transport. CBV influx was slow, saturable, strongly inhibited by adenine or hypoxanthine, and occurred via both the nucleobase carrier (V_{max} = 0.67 pmol/s/μl cell water; K_m = 50 μM) and the nucleoside carrier (V_{max} = 0.47 pmol/s/μl cell water; K_m = 440 μM). Similar qualitative results were obtained with CD4$^+$ CEM cells, although CBV influx rates were somewhat higher and abacavir influx rates lower, compared to the corresponding rates in erythrocytes. Equilibrium studies further revealed that both compounds are concentrated intracellularly, but nonmetabolically, in both cell types, apparently due to cytosolic protein binding (absent in erythrocyte ghosts). We conclude that, in both cell types, while CBV influx is slow and carrier-dependent, abacavir influx occurs rapidly by nonfacilitated diffusion. The membrane permeation characteristics of abacavir are consistent with its superior oral bioavailability and its impressive ability to penetrate the central nervous system.

Keywords: Drug transport; Influx kinetics; Nonfacilitated diffusion; HIV; Abacavir; Erythrocyte ghosts

1. Introduction

Abacavir, (−)-(1*S*,4*R*)-4-[2-amino-6-(cyclopropylamino)-9*H*-purin-9-yl]-2-cyclopentene-1-methanol (Fig. 1), is a novel purine carbocyclic nucleoside analogue that exhibits potent and selective activity against HIV-1 and HIV-2 [1]. The hemisulfate salt of this compound has been evaluated clinically as an anti-HIV agent [2–7] and has received approval by the FDA for the treatment of HIV (as Ziagen™ [abacavir sulfate] and, more recently, as part of the anti-HIV triple combination tablet, Trizivir™). Abacavir shares structural similarity with CBV, the first carbocyclic nucleoside reported to have anti-HIV activity [8], differing at the 6-position of the purine ring, where abacavir contains a cyclopropylamino moiety instead of the 6-lactam

Abbreviations: Abacavir, (−)-(1*S*,4*R*)-4-[2-amino-6-(cyclopropylamino)-9*H*-purin-9-yl]-2-cyclopentene-1-methanol (Ziagen™; [abacavir sulfate] previously known as 1592U89); AZT, 3′-azido-3′-deoxythymidine; CBV, (−)-carbovir (9-[4α-(hydroxymethyl)cyclopent-2-ene-1α-yl]guanine); CNS, central nervous system; *ei*, equilibrative nucleoside transporter that is insensitive to inhibition by NBMPR; *es*, equilibrative nucleoside transporter that is sensitive to inhibition by nM concentrations of NBMPR; Hepes, 4-(2-hydroxyethyl)-1-piperazineethanesulfonic acid; HIV-1, human immunodeficiency virus type 1; HIV-2, human immunodeficiency virus type 2; HPLC, high-performance liquid chromatography; NBMPR, nitrobenzylthioinosine; 5P8, 5.0 mM sodium phosphate (pH 8.0); 5P8-SS, 5P8 containing 0.09% NaCl and 10% sucrose.

* Corresponding author. Tel.: +1 919 483 2095; fax: +1 919 483 6053.
E-mail address: susan.m.daluge@gsk.com (S.M. Daluge).

0006-2952/$ – see front matter © 2004 Elsevier Inc. All rights reserved.
doi:10.1016/j.bcp.2004.06.025

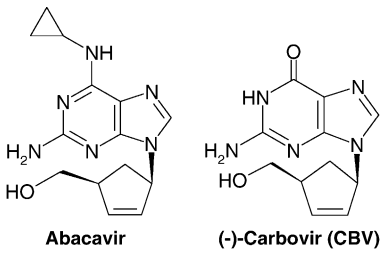

Fig. 1. Chemical structures of abacavir and CBV.

functionality of CBV (Fig. 1). Like CBV, abacavir is metabolized intracellularly to carbovir triphosphate [9,10]; CBV triphosphate can then potently and selectively inhibit HIV reverse transcriptase, without significant inhibition of human DNA polymerases or DNA primase [1,11,12]. In anabolic studies using human T-lymphoblastoid $CD4^+$ CEM cells, Faletto et al. [10] showed that the formation of CBV triphosphate from abacavir did not involve the intermediate formation of CBV but rather proceeded through the direct phosphorylation of abacavir, followed by a dealkylamination step at the monophosphate level.

Abacavir has been found to be superior to CBV both in its pharmacokinetics and in its ability to penetrate the CNS [4,13–15]. We have previously shown that the membrane permeation of CBV in human erythrocytes (at 37 °C) is very slow and is dependent upon facilitated diffusion, primarily via the nucleobase carrier but also to a small extent via the *es* nucleoside transporter [16]. Because membrane permeation is an important determinant of drug pharmacology, we have compared the membrane permeation characteristics of abacavir and CBV in human erythrocytes and in human T-lymphoblastoid $CD4^+$ CEM cells.

In this report, we describe dramatic differences in both the kinetics and the mechanism of influx of these carbocyclic nucleoside analogues in the two types of human cells. Also, we demonstrate that both abacavir and CBV are concentrated in these cells and provide evidence suggesting that this effect is attributable to cytosolic protein binding of these agents following cellular uptake. We also describe the development of a novel preparation of "sucrose-dense" erythrocyte ghosts which sediment through an oil phase.

2. Materials and methods

2.1. Materials

Abacavir [1] and CBV [16] were synthesized in these laboratories; purity levels were >99% as determined by reversed-phase high-performance liquid chromatography [17]. Adenine, hypoxanthine, NBMPR, papaverine hydrochloride, sucrose, mannitol, and 1-bromododecane were purchased from Sigma. Dow Corning 550 silicone fluid was obtained from Dow Corning Corp. Dilazep was kindly provided from Hoffmann-La Roche. Hepes and RPMI-1640 were obtained from GIBCO. [^{3}H]Abacavir (1.6 Ci/mmol) and [^{3}H]CBV (2 Ci/mmol) were radiolabeled by Moravek Biochemicals, Inc. [Methyl-^{3}H]dThd (83 Ci/mmol) was from Amersham Corp. Purity levels of radiolabeled permeants used in these studies were >97% as determined by reversed-phase HPLC. [U-^{14}C]Sucrose (4 Ci/mol) and ^3H_2O (1 mCi/g) were purchased from Du Pont-New England Nuclear.

2.2. Preparation of human erythrocytes

Erythrocytes were isolated from blood collected from healthy human volunteers and washed three times with ice-cold Hepes/saline (10 mM Hepes, pH 7.3, in physiological saline). Cells were resuspended in this buffered saline (± potent inhibitors of nucleoside transport) to a hematocrit of 20–25% [18] for use in transport assays.

2.3. Preparation of novel "sucrose-dense" human erythrocyte ghosts

The traditional ghost preparation described by Steck and Kant [19] was modified so that ghosts were resealed in the presence of 10% (293 mM) sucrose (instead of physiological saline) resulting in relatively dense ghosts; 10% physiological saline (i.e., 0.09% NaCl) was retained in this resealing solution to satisfy the ionic strength requirement for complete resealing.

Freshly isolated human erythrocytes were washed three times with a cold solution of 150 mM NaCl and 5 mM sodium phosphate, pH 8.0. After the final wash, cells were centrifuged at low speed (500 × *g*) for 10 min and the supernatant was discarded. Cells were lysed by the rapid addition of, and mixing with, 50 volumes of a cold solution of 5 mM sodium phosphate, pH 8.0 (5P8). The lysate was centrifuged at high speed (22,000 × *g* for 10 min). The supernatant was discarded and the centrifuge tube rotated on its axis so that the loose membranous pellet – constituting unsealed ghosts – slid away from a small hard button pellet; this latter pellet was aspirated away leaving only the loose, pink pellet of unsealed ghosts. Ghosts were washed with cold 5P8 (≈50 volumes) and, following another high-speed centrifugation, were recovered as a loose, milk-white pellet.

Washed, unsealed erythrocyte ghosts were incubated at 37 °C with 50 volumes of 10% sucrose and 0.09% NaCl in 5 mM sodium phosphate, pH 8.0 (5P8-SS). The ghosts were pelleted (22,000 × *g* for 10 min) and washed twice more: first with cold 5P8-SS, and then with a cold solution of 5P8-SS with pH readjusted to 7.3. After the final centrifugation, the supernatant was discarded and sealed "sucrose-dense" ghosts were recovered. This final loose pellet constituted a ghost suspension of ≈25% (as determined with a hematocrit centrifuge). These "dense ghosts" were uniquely compatible for use in "oil-stop" transport assays and allowed assessment of uptake equilibrium in the

absence of cytosolic proteins. Typically, this ghost suspension, stored at 4 °C, was used in transport assays performed within 24 h of the ghost preparation, although the stability of these ghosts appeared to extend for at least several days. All prepared sucrose solutions were routinely filter-sterilized and capped to minimize bacterial contamination.

2.4. Preparation of CD4$^+$ CEM cells

A line of high-CD4$^+$-expressing human T-lymphoblastoid CEM cells was obtained from the National Institutes of Health AIDS Research and Reference Reagent Program. Cells were maintained in exponential growth in RPMI-1640 medium containing 2 mM L-glutamine and 10% fetal bovine serum at 37 °C with 5% CO_2 in a humidified incubator. Harvested CD4$^+$ CEM cells were washed three times by centrifugation and resuspension in RPMI-1640 medium containing 10 mM Hepes, pH 7.3 [20]. Cells were resuspended to a final cell density of $\approx 10^8$ cells/ml for use in transport assays.

2.5. Initial rates of influx

[^{3}H]Abacavir and [^{3}H]CBV influx in human erythrocytes was measured at 20 °C in Hepes/saline using the "papaverine-stop" assay method [18]. Two persons performed these assays together: one to initiate and the other to stop the assay; an electronic clock was replaced by a metronome in the timing of short ($\leq$1 min) assay times. Each assay was initiated by the addition of 80 μl of radiolabeled permeant (± test inhibitor) to 20 μl of cell suspension (± potent inhibitor of nucleoside transport: dilazep or NBMPR). Assays were terminated by addition of 700 μl of an ice-cold saturated solution of papaverine HCl in saline followed by 400 μl of ice-cold *n*-bromododecane. Erythrocytes were microcentrifuged through the oil phase away from contaminating aqueous assay medium within 8 s after adding the cold papaverine to minimize post-quench leakage of abacavir across the membrane. Influx rates, expressed as pmol/s/μl cell water, were determined by linear regression analysis of plots of cell-associated radiolabeled permeant versus assay time over the initial linear phase of influx (commonly referred to as zero-trans influx: i.e., that brief, initial time interval where movement across the membrane is virtually unidirectional into the cell). Each influx rate determination was based on influx measurements from at least five assay times. For abacavir influx, zero-trans influx was monitored at assay times of 0, 0.3, 0.6, 0.9, and 0.9 s (duplicate time point) (metronome setting = 208 tones/min). For CBV influx, a saturable process [16], zero-trans influx was monitored at assay times of 0, 2, 4, 6, and 7 s at low ($\leq$20 μM) concentrations and 0, 30, 60, 90, and 120 s at high ($\geq$2 mM) concentrations.

[^{3}H]Abacavir and [^{3}H]CBV influx at 20 °C in human T-lymphoblastoid CD4$^+$ CEM cells was similarly measured except: (i) assay stock solutions were prepared in RPMI-1640 medium containing 10 mM Hepes, pH 7.3; (ii) each assay was initiated by the addition of 50–70 μl of radiolabeled permeant to 50–30 μl of cell suspension ($\approx 10^8$ cells/ml), to yield a final assay volume of 100 μl; and (iii) a less dense oil (relative to *n*-bromododecane) consisting of 96% *n*-bromododecane:4% silicone fluid was added to the assay mixture just before the microcentrifugation step. In these cells, initial influx rates were calculated based on at least six timed measurements of influx: 0, 1, 2, 3, 4, and 5 s assay times were used for abacavir influx and for the influx of subsaturating concentrations of CBV; at higher (saturating) CBV concentrations, longer assay times (up to 60 s) were used.

2.6. Kinetic analyses

For CBV influx in erythrocytes, where two saturable systems were identified [16], influx kinetic parameters were determined by nonlinear regression [21] with the equation $v = (V_{max1})(S)/(S + K_{m1}) + (V_{max2})(S)/(S + K_{m2})$ using a $1/v^2$ weighting factor [22]. For CBV influx in CD4$^+$ CEM cells, where only a single saturable system was indicated, influx kinetic parameters were determined by directly fitting the data to a hyperbola according to the method of Wilkinson [23] and the computer program of Cleland [24]. For abacavir influx, where nonfacilitated diffusion was the only permeation pathway detected, a rate constant was calculated based on the linear regression analysis of the plot of influx rate versus permeant concentration [25].

2.7. Uptake equilibrium studies

Time-dependent permeant uptake was measured to equilibrium using a modification [18] of the traditional "oil-stop" assay method [26]. With erythrocytes and CD4$^+$ CEM cells, assay conditions were as described above for initial rate measurements (using assay volumes of 100 or 200 μl), except that the papaverine addition was omitted. Instead, assay termination was defined as the time at which the microcentrifuge was started in the process of physically pelleting cells through the oil layer and away from the less dense, aqueous assay medium that remains above the oil layer.

Equilibrium uptake studies of radiolabeled permeants with the "sucrose-dense" erythrocyte ghosts were conducted in a similar manner but with the following modifications. All radiolabeled permeant stock solutions were made up in 293 mM mannitol and 0.09% NaCl in 5 mM sodium phosphate, pH 7.3. These solute concentrations are thus identical to those present during the re-sealing of the washed, lysed ghosts; the single and notable difference between the intra- and extracellular contents is that 293 mM sucrose (molecular weight = 342) is sealed inside the ghosts, while 293 mM mannitol (molecular weight = 182), which is less dense than equimolar sucrose, is present

extracellularly. Since both mannitol and sucrose traverse cell membranes poorly, isotonicity across the ghost membrane (and, thus, ghost stability) is preserved. Concurrently and importantly, the relatively dense ghosts can be centrifuged through an oil layer and away from the less dense extracellular media. In these uptake assays, 180 μl of radiolabeled permeant was added to 20 μl of ghost suspension (≈25%) to initiate uptake; assay termination was defined as the start of a 30-s microcentrifugation that sedimented the dense ghosts through a 20 °C oil mixture of 96% *n*-bromododecane:4% silicone fluid[1] (that was added to the assay mixture just prior to starting the microcentrifuge). A tightly packed, clean white ghost pellet was formed below the oil phase with the aqueous assay medium retained above.

Intracellular volumes (referred to as "water spaces") for erythrocytes, erythrocyte ghosts, and $CD4^+$ CEM cells were determined in each experiment by using ^3H_2O in place of the radiolabeled permeant with the "oil-stop" assay [16]. [^{14}C]Sucrose was used to correct for the relatively small extracellular radioactivity that carried through the oil layer as part of the cell (or ghost) pellet following the microcentrifugation step.

2.8. Metabolism

Metabolism studies were based on cellular incubations of radiolabeled permeant using conditions defined in the oil-stop assay method described above, except that, following centrifugation of the cells through the oil layer, the cellular contents were extracted with cold acetonitrile [27] and then analyzed by C_{18} reversed-phase HPLC [17].

3. Results

3.1. Uptake equilibrium studies of permeants with human erythrocytes, erythrocyte ghosts, and $CD4^+$ CEM cells

The time-dependent influx of 5 μM concentrations of [^{3}H]abacavir and [^{3}H]CBV at 20 °C is shown in human erythrocytes (Fig. 2A), in erythrocyte ghosts (Fig. 2B), and in $CD4^+$ CEM cells (Fig. 2C). The uptake of both abacavir and CBV into erythrocytes reached equilibration within 3 min; at equilibrium, intracellular permeant concentrations were substantially higher than extracellular concentrations: by 3.2- to 3.8-fold for abacavir and by 1.8- to 2.2-fold for CBV. In parallel incubations with $CD4^+$ CEM cells, the uptake of both abacavir and CBV attained equilibrium within 2 min, by which time intracellular concentrations of these permeants were approximately 1.7-fold higher than their extracellular concentrations. Additional experiments at millimolar permeant concentrations revealed the same qualitative and quantitative concentrative effects in both cell types. These unexpected and dramatic concentrative effects for abacavir and CBV were not observed following incubations with erythrocyte ghost preparations (Fig. 2B). By contrast, [^{3}H]dThd equilibrated very rapidly within erythrocytes and ghosts to its extracellular concentration (Fig. 2A and B); [^{3}H]dThd influx was not investigated in $CD4^+$ CEM cells.

3.2. Metabolism of abacavir and CBV

The possible metabolism of 10 μM or 10 mM [^{3}H]abacavir in human erythrocytes was investigated after 10-min incubations at 20 °C. With both concentrations, ≥99% of the cell-associated radioactivity was eluted from the reversed-phase C_{18} HPLC column at the same retention time as authentic abacavir standard. CBV has been shown previously not to be metabolized by human erythrocytes [16]. In similar experiments, ≥99% of cellular radioactivity was found unchanged after 20- and 60-min $CD4^+$ CEM cellular incubations with both low (10 μM) and high (1.0 mM) concentrations of [^{3}H]abacavir or [^{3}H]CBV (data not shown).

3.3. Initial influx rates

The ability of the "papaverine-stop" assay method to measure initial influx rates of abacavir and CBV in erythrocytes (20 μM permeant) and in $CD4^+$ CEM cells (40 μM permeant) is demonstrated in Fig. 3. Abacavir influx in erythrocytes was linear to only 1.0 s and was much faster (23-fold) than that of CBV. A substantial influx rate advantage of abacavir over CBV was also observed in $CD4^+$ CEM cells, especially at higher permeant concentrations (Fig. 4).

3.4. Concentration-dependence of influx rates

The relationship between influx rate and permeant concentration for both abacavir and CBV in erythrocytes and in $CD4^+$ CEM cells is presented in Fig. 4. In both cell types, abacavir influx rates were linearly dependent on concentration, allowing for the straightforward calculation of a nonfacilitated diffusion rate constant (pmol/s/mM/μl cell water). In contrast, CBV influx in both erythrocytes and $CD4^+$ CEM cells exhibited saturable kinetics.

3.5. Effects of inhibitors on permeant influx

To further characterize the mechanism of permeation for abacavir, various potential inhibitors were tested against the influx of low (7–10 μM) and high (1.0 mM) concen-

[1] Although beyond the scope of this report, we have validated the use of these "sucrose-dense" ghosts in a "papaverine-stop" assay that is based on the same assay conditions described for human erythrocytes. In these assays, permeant flux across the erythrocyte ghost membrane was quenched with our standard ice-cold papaverine (containing saline) addition, and ghosts were microcentrifuged through an oil layer. Since both the oil and papaverine that are added to the assay are ice-cold, we used a 90:10 ratio of *n*-bromododecane:silicone fluid to maintain a similar oil density as that described in the 20 °C oil-stop assay.

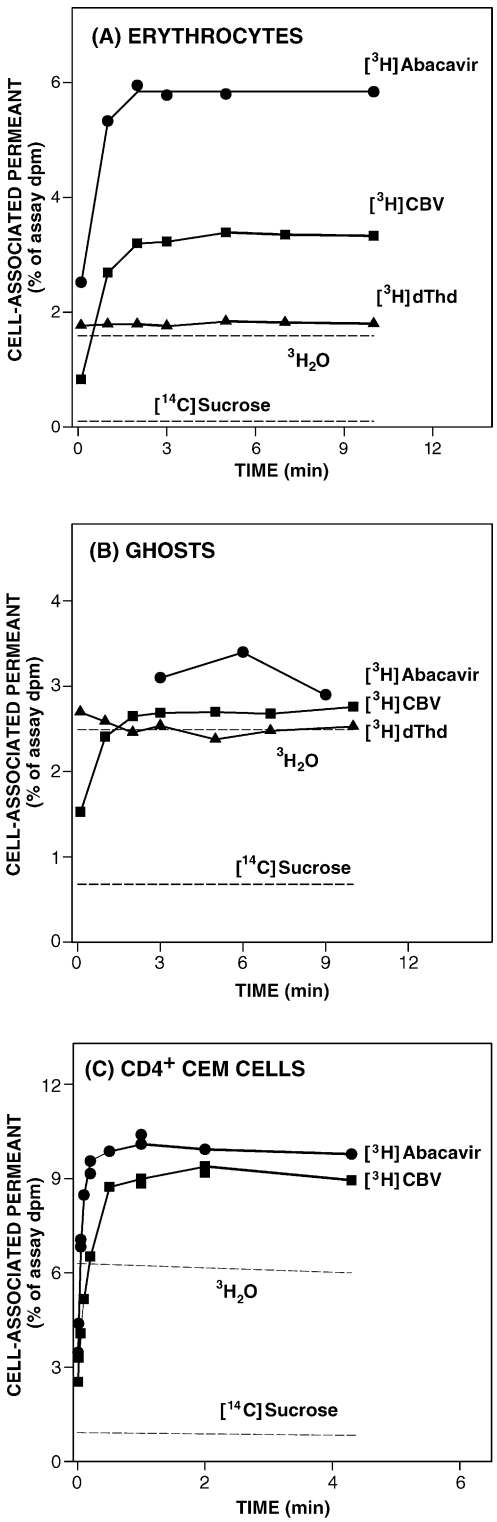

Fig. 2. Uptake equilibrium studies in (A) human erythrocytes, (B) human erythrocyte ghosts, and (C) $CD4^+$ CEM cells. Human erythrocytes (5 μl of packed cells) or erythrocyte ghosts (5 μl of packed ghosts) were incubated for the indicated times at 20 °C with 5.0 μM [^{3}H]abacavir (1.1 Ci/mmol) (*circles*), 5.0 μM [^{3}H]CBV (0.68 Ci/mmol) (*squares*), or 5.0 μM [^{3}H]dThd (0.57 Ci/mmol) (*triangles*) prior to assay termination by the "oil-stop" method and determination of cell-associated radioactivity as described under "Experimental Procedures." $CD4^+$ CEM cells (2×10^6 cells) were similarly incubated for the indicated times at 20 °C with 10 μM [^{3}H]abacavir (0.37 Ci/mmol) (*circles*) or 10 μM [^{3}H]CBV (0.50 Ci/mmol) (*squares*) prior to determination of cell-associated radioactivity. Intracellular ^3H_2O space is represented by the upper dashed lines, and extracellular [^{14}C]sucrose space by the lower dashed lines.

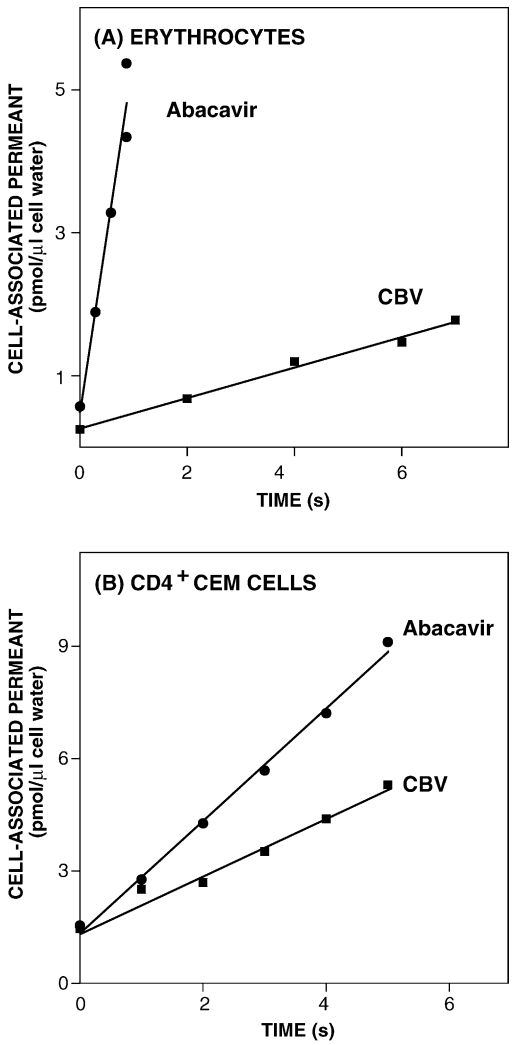

Fig. 3. Initial rates of influx of abacavir and CBV in (A) human erythrocytes and (B) $CD4^+$ CEM cells. Human erythrocytes (5 μl of packed cells) were incubated for the indicated times at 20 °C with 20 μM [^{3}H]abacavir (70 Ci/mol) (*circles*) or 20 μM [^{3}H]CBV (170 Ci/mol) (*squares*) prior to assay termination by the "papaverine-stop" method and determination of cell-associated radioactivity as described under "Experimental Procedures." $CD4^+$ CEM cells (4×10^6 cells) were incubated for the indicated times at 20 °C with 40 μM [^{3}H]abacavir (13 Ci/mol) (*circles*) or 40 μM [^{3}H]CBV (18 Ci/mol) (*squares*) prior to determination of cell-associated radioactivity.

trations of abacavir and CBV in both erythrocytes (Table 1) and $CD4^+$ CEM cells (Table 2). Potent inhibitors of nucleoside transport (NBMPR, dilazep) were without effect on abacavir influx into either cell type. However, high, supraphysiological concentrations (1.0–3.0 mM) of adenine appeared to inhibit the influx of low concentrations of abacavir (7.0 μM) to a small and marginally detectable extent in erythrocytes; in $CD4^+$ CEM cells, no statistically significant inhibition of abacavir influx by either adenine or hypoxanthine was detected. This contrasted sharply with

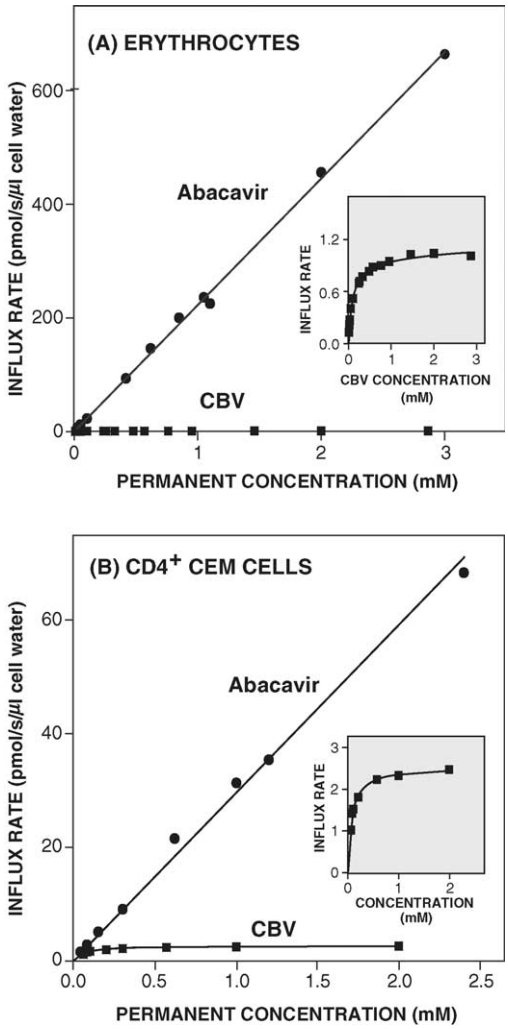

Fig. 4. Concentration dependence of abacavir and CBV influx rates in (A) human erythrocytes and (B) $CD4^+$ CEM cells. The influx of [^{3}H]abacavir (5.3 and 52 Ci/mol with erythrocytes; 12 and 140 Ci/mol with $CD4^+$ CEM cells) (*circles*) and [^{3}H]CBV (18 Ci/mol with erythrocytes; 13 Ci/mol with $CD4^+$ CEM cells) (*squares*) influx was assayed at 20 °C, and initial velocities of influx were determined as described under "Experimental Procedures." *Insets*: expanded scale of the CBV data.

the inhibition profiles observed with CBV influx. Consistent with previous observations from experiments performed at 37 °C [16], the influx of CBV in erythrocytes at 20 °C was almost completely inhibited by adenine at low CBV concentrations and was inhibited significantly by both adenine and nucleoside transport inhibitors at 1.0 mM CBV. The preferential inhibition of CBV influx by nucleoside transport inhibitors at high permeant concentrations (e.g., 1.0 mM) would be predicted by the kinetic parameters of this two-carrier system summarized in Table 3, because the contribution of the nucleoside carrier to CBV influx would be measurable only at high CBV concentrations. Unexpectedly, no inhibition of CBV influx into $CD4^+$ CEM cells was detected in the presence of NBMPR at either high or low permeant concentration (Table 2). This was confirmed in an additional experiment using these cells where the influx of a higher concentration

Table 1
Effects of nucleoside transport inhibitors, thymidine, and adenine on the influx of abacavir and CBV in human erythrocytes at 20 °C[a]

Inhibitor(s)	Percent inhibition of permeant influx			
	[^{3}H]Abacavir		[^{3}H]CBV	
	7 μM	1.0 mM	7 μM	1.0 mM
NBMPR (4.0 μM)	11	14	9	27*
Dilazep (4.0 μM)	4	0	11	25*
dThd (1.0 mM)	18	9	17	34*
Adenine (1.0 mM)	25*	9	94*	74*
Adenine (3.0 mM)	25*	13	97*	83*
Adenine (3.0 mM) + NBMPR (4.0 μM)	18	0	98*	95*
Adenine (3.0 mM) + dilazep (4.0 μM)	21	6	99*	95*

[a] Control influx rates (pmol/s/μl cell water) were 1.6 (7.0 μM abacavir); 210 (1.0 mM abacavir); 0.14 (7.0 μM CBV); and 1.4 (1.0 mM CBV).
* Inhibited rate significantly different from control rate, $P < 0.05$.

of CBV (1.6 mM) was assessed in the presence of 1.0 mM adenine versus the combination of 1.0 mM adenine and 1.0 μM NBMPR; under both conditions, the same inhibition of CBV influx (68%) was measured.

3.6. Kinetic parameters of influx

Kinetic parameters for the influx of abacavir and CBV in both cell types are summarized in Table 3. The nonfacilitated diffusion rate constant for abacavir influx was 7.4-fold greater in erythrocytes (200 pmol/s/mM/μl cell water) than in $CD4^+$ CEM cells (27 pmol/s/mM/μl cell water). Plots of abacavir influx rate versus abacavir concentration for both cell types were strictly linear over the entire concentration range of permeant (Fig. 4), suggesting that nonfacilitated diffusion is the sole significant permeation mechanism. This is consistent with the lack of evidence from inhibition studies (Tables 1 and 2) for a detectable secondary, carrier-mediated component of membrane permeation and validates the use of a simple rate to completely

Table 2
Effects of NBMPR, adenine, and hypoxanthine on the influx of abacavir and CBV in $CD4^+$ CEM cells at 20 °C[a]

Inhibitor(s)	Percent inhibition of permeant influx			
	[^{3}H]Abacavir		[^{3}H]CBV	
	10 μM	1.0 mM	10 μM	1.0 mM
NBMPR (3.0 μM)	5	0	1	1
Adenine (1.0 mM)	25	0	96*	79*
Hypoxanthine (1.0 mM)	2	0	88*	50*
Adenine (1.0 mM) + hypoxanthine (1.0 mM)	23	1	96*	74*
Adenine (1.0 mM) + hypoxanthine (1.0 mM) + NBMPR (3.0 μM)	22	7	99*,b	85*,b

[a] Control influx rates (pmol/s/μl cell water) were 0.35 (10 μM abacavir); 30 (1.0 mM abacavir); 0.24 (10 μM CBV); and 1.9 (1.0 mM CBV).
[b] Not significantly different from the "+ adenine" or the "+ adenine + hypoxanthine" conditions.
* Inhibited rate significantly different from control rate, $P < 0.05$.

Table 3
Kinetic parameters for the influx of abacavir and CBV in human erythrocytes and CD4+ CEM cells at 20 °C

	Human erythroctyes		CD4+ CEM cells	
	Abacavir	CBV	Abacavir	CBV
Nucleobase carrier				
K_m (μM)	nd[a]	50 ± 10	nd	75 ± 5
V_{max} (pmol/s/μl cell water)	nd	0.67 ± 0.14	nd	2.4 ± 0.6
Nucleoside carrier				
K_m (μM)	nd	440 ± 200	nd	nd
V_{max} (pmol/s/μl cell water	nd	0.47 ± 0.11	nd	nd
Nonfacilitated diffusion				
Rate constant (pmol/s/mM/μl cell water)	200 ± 30	nd	27 ± 6	nd

[a] Not detectable.

define the kinetics of abacavir influx. In contrast, the saturation curves describing CBV influx revealed no measurable nonfacilitated diffusion occurring in either cell type. In erythrocytes, the concentration-dependent rate curve for CBV influx at 20 °C was a good fit to the same two-carrier model (Table 3) that was described previously from CBV transport studies performed at 37 °C [16]; influx kinetic parameters in this study are consistent (and predictably lower, given assay temperatures of 20 °C versus 37 °C) with the previously reported influx K_m and V_{max} determinations [16]. However, in CD4+ CEM cells the saturation curve for CBV influx is consistent with only a single significant permeation pathway: the nucleobase carrier. As shown in Table 3, similar influx K_m values characterize the interaction of CBV with the nucleobase carrier in each of the two different cell types. Whether the higher V_{max} for CBV influx determined with CD4+ CEM cells versus erythrocytes is due to higher turnover of the carrier or to a higher density of carriers on the cell surface cannot be resolved from these studies.

4. Discussion

The present investigation demonstrates, in two different types of human cells, the superior membrane permeation characteristics of abacavir relative to those of CBV and provides a detailed biochemical understanding of the differing mechanisms by which these two structurally related carbocyclic nucleosides enter cells.

Abacavir was found to enter both human erythrocytes and CD4+ CEM cells exclusively by nonfacilitated diffusion. This conclusion is based upon the linear relationship of influx rate to abacavir concentration (Fig. 4) and upon low-to-absent inhibition of abacavir influx by inhibitors or permeants of either the *es* nucleoside transporter or the nucleobase transporter present in these two cell types (Tables 1 and 2). It is of interest to note that human erythrocytes [28] and CEM cells [29] contain only the NBMPR-sensitive *es* nucleoside transporter and neither the *ei* nor any of the Na^+-dependent nucleoside transporters. These membrane permeation characteristics of abacavir contrasted markedly with those of CBV, which exhibited saturable kinetics of influx (Fig. 4) and strong inhibition of influx by adenine (Tables 1 and 2), a high-affinity permeant of the nucleobase carrier [18].

The marked differences in membrane permeation characteristics observed between abacavir and CBV can be attributed to differences in their physicochemical properties. Replacement of the 6-lactam moiety of CBV with the cyclopropylamino group of abacavir (Fig. 1) results in a greatly increased octanol:water partition coefficient for abacavir (15.4) compared to that for CBV (0.29) [1]. A previous study has shown that replacement of the 3′-hydroxyl moiety of dThd with the lipophilic azido group (to give AZT) resulted in a complete change from carrier-mediated transport of thymidine to nonfacilitated diffusion of AZT [30]. Moreover, analogous to a previous comparison between desciclovir and acyclovir [25], removal of the hydrogen bond-forming 6-lactam moiety of CBV would, in itself, be expected to reduce the energy of desolvation and to consequently impart to abacavir an increased tendency to permeate cell membranes by nonfacilitated diffusion. The contribution of desolvation energy in determining rates of nonfacilitated diffusion of other nucleoside analogues has been discussed previously [31–33].

The relatively high lipophilicity of abacavir and its resultant carrier-independent permeation of membranes provides an understanding for the much more rapid passage of abacavir across cell membranes relative to CBV. The large dependence of CBV upon the limiting nucleobase carrier for membrane permeation results in a kinetic barrier for cellular uptake. Moreover, whereas physiological nucleobases can compete with CBV for transport into cells via the nucleobase carrier, no definitive inhibitory effect of these endogenous nucleobases is observed on the membrane permeation of abacavir (Tables 1 and 2).

Equilibrium uptake experiments with both erythrocytes and CEM cells provided evidence of apparently concentrative transport of abacavir (up to 3- to 4-fold) and CBV (~1.7-fold) in these cells (Fig. 2A and C). This cellular accumulation of radiolabeled permeants was shown not to be the result of metabolic conversion of these nucleoside analogues into substances (e.g., nucleotides) which would

have been trapped intracellularly. The remaining, most likely explanations for this phenomenon were either membrane adsorption or binding to intracellular proteins. In an attempt to distinguish between these latter two possibilities, we devised a novel preparation of ''sucrose-dense'' erythrocyte ghosts which could be centrifuged through an oil phase and which, therefore, allowed equilibrium uptake studies in the absence of intracellular proteins. By contrast with native erythrocytes, these ''sucrose-dense'' erythrocyte ghosts exhibited very little concentration of either abacavir or CBV at equilibrium (Fig. 2B). These results suggest strongly that the unexpected magnitude of abacavir and CBV uptake observed with native erythrocytes is attributable to the binding of these nucleoside analogues to intracellular proteins following their permeation of the cell membrane.

Results obtained with abacavir in this investigation add to previous data indicating that CEM cells, relative to human erythrocytes, exhibit greatly reduced rates of nonfacilitated diffusion by several compounds. The rate constant of nonfacilitated diffusion for AZT in CEM cells (3.9 pmol/s/mM/μl cell water) [20] was much lower than that observed in erythrocytes (29.7 pmol/s/mM/μl cell water) [30]. 5-Chloro-2′,3′-dideoxy-3′-fluoruridine exhibited rate constants of nonfacilitated diffusion of 2.8 pmol/s/mM/μl cell water in CEM cells [20] and 25 pmol/s/mM/μl cell water in erythrocytes (B.A. Domin, unpublished observation). Similarly, the rate constant of nonfacilitated diffusion for 2′,3′-dideoxy-2,6-diaminopurine ribonucleoside in CEM cells (3.3 pmol/s/mM/μl cell water) was considerably lower than that in erythrocytes (23 pmol/s/mM/μl cell water) [34]. Even though erythrocytes contain approximately 2.3-fold greater surface area per μl of cell water than CEM cells, CEM cells still consistently yielded lower normalized rate constants for nonfacilitated diffusion. These differences indicate that the membrane composition of CEM cells is less favorable for the nonfacilitated permeation of small, lipophilic molecules than is the membrane of human erythrocytes. Whether this difference reflects a difference in cell type (i.e., erythrocytes versus lymphocytes), a difference in cell history (i.e., freshly isolated cells versus cells grown in culture), or a difference in malignant status (i.e., nonmalignant versus malignant) cannot be ascertained from the limited existing data.

The pharmacological properties of abacavir are remarkably superior to those of CBV in many respects, perhaps most notably with respect to pharmacokinetics and to penetration of the CNS [4,12–15]. This latter characteristic – i.e., superior CNS penetration by abacavir – may be especially critical in light of data recently presented by Lanier et al. [35] suggesting that viral suppression in the periphery may be inadequate if it is not also accompanied by viral suppression in the CNS. Both nucleoside analogues are ultimately metabolized to the same intracellular antiviral nucleotide, CBV triphosphate. However, abacavir realizes this metabolic transformation by unique cellular membrane transport *and* intracellular metabolic pathways [1,10]. Following membrane permeation and subsequent monophosphorylation, the dealkylamination reaction that metabolically converts abacavir monophosphate to CBV monphosphate occurs intracellularly, effectively preventing release of free CBV into the circulation and thereby avoiding the toxicity associated with CBV [1,10]. The superior oral bioavailability and CNS penetration of abacavir, relative to CBV, is consistent with the ability of the much more lipophilic abacavir to permeate cell membranes, at a high rate, by nonfacilitated diffusion. In this regard, it is notable that lipophilic AZT also enters cells by nonfacilitated diffusion [30] and shares with abacavir these same dual characteristics of high oral bioavailability and significant CNS penetration [36]. However, abacavir is demonstrably much more efficient (6.7- to 6.9-fold) than AZT in permeating cell membranes by nonfacilitated diffusion.

Acknowledgements

The authors thank Barbara J. Rutledge, Ph.D., for editing assistance.

References

[1] Daluge SM, Good SS, Faletto MB, Miller WH, St. Clair MH, Boone LR, et al. 1592U89, a novel carbocyclic nucleoside analog with potent, selective anti-human immunodeficiency virus activity. Antimicrob Agents Chemother 1997;41:1082–93.

[2] Saag MS, Sonnerborg A, Torres RA, Lancaster D, Gazzard BG, Schooley RT, et al. Antiretroviral effect and safety of abacavir alone and in combination with zidovudine in HIV-infected adults. AIDS 1998;12:F203–9.

[3] Hughes W, McDowell JA, Shenep J, Flynn P, Kline MW, Yogev R, et al. Safety and single-dose pharmacokinetics of abacavir (1592U89) in human immunodeficiency virus type 1-infected children. Antimicrob Agents Chemother 1999;43:609–15.

[4] Kumar PN, Sweet DE, McDowell JA, Symonds W, Lou Y, Hetherington S, et al. Safety and pharmacokinetics of abacavir (1592U89) following oral administration of escalating single doses in human immunodeficiency virus type 1-infected adults. Antimicrob Agents Chemother 1999;43:603–8.

[5] Staszewski S, Katlama C, Harrer T, Massip P, Yeni P, Cutrell A, et al. A dose-ranging study to evaluate the safety and efficacy of abacavir alone or in combination with zidovudine and lamivudine in antiretroviral treatment-naive subjects. AIDS 1998;12:F197–202.

[6] McMahon D, Lederman M, Haas DW, Haubrich R, Stanford J, Cooney E, et al. Antiretroviral activity and safety of abacavir in combination with selected HIV-1 protease inhibitors in therapy-naive HIV-1-infected adults. Antivir Ther 2001;6:105–14.

[7] Kessler HA, Johnson J, Follansbee S, Sension MG, Mildvan D, Sepulveda GE, et al. Abacavir expanded access program for adult patients infected with human immunodeficiency virus type 1. Clin Infect Dis 2002;34:535–42.

[8] Vince R, Hua M, Brownell J, Daluge SM, Lee FC, Shannon WM, et al. Potent and selective activity of a new carbocyclic nucleoside analog (carbovir: NSC 614846) against human immunodeficiency virus in vitro. Biochem Biophys Res Commun 1988;156:1046–53.

[9] Bondoc Jr LL, Shannon WM, Secrist III JA, Vince R, Fridland A. Metabolism of the carbocyclic nucleoside analogue carbovir, an inhibitor of human immunodeficiency virus, in human lymphoid cells. Biochemistry 1990;29:9839–43.
[10] Faletto MB, Miller WH, Garvey EP, St. Clair MH, Daluge SM, Good SS. Unique intracellular activation of the potent anti-human immunodeficiency virus agent 1592U89. Antimicrob Agents Chemother 1997;41:1099–107.
[11] White EL, Parker WB, Macy LJ, Shaddix SC, McCaleb G, Secrist III JA, et al. Comparison of the effect of carbovir, AZT, and dideoxynucleoside triphosphates on the activity of human immunodeficiency virus reverse transcriptase and selected human polymerases. Biochem Biophys Res Commun 1989;161:393–8.
[12] Parker WB, White EL, Shaddix SC, Ross LJ, Buckheit RW, Germany JM, et al. Mechanism of inhibition of human immunodeficiency virus type 1 reverse transcriptase and human DNA polymerases alpha, beta, and gamma by the 5′-triphosphates of carbovir, 3′-azido-3′-deoxythymidine, 2′,3′-dideoxyguanosine, and 3′-deoxythymidine: a novel RNA template for the evaluation of antiretroviral drugs. J Biol Chem 1991;266:1754–62.
[13] Good SS, Owens BS, Faletto MB, Mahony WB, Domin BA. Disposition in monkeys and mice of (1*S*,4*R*)-4-[2-amino-6-(cyclopropylamino)-9*H*-purin-9-yl]-2-cyclopentene-1-methanol (1592U89). Abstracts of the 34th Interscience Conference on Antimicrobial Agents and Chemotherapy; 1994. p. 92 (poster abstract I86).
[14] Huang S-H, Remmel RP, Zimmerman CL. The bioavailability and nonlinear clearance of (−)-carbovir in the rat. Pharm Res 1991;8:739–43.
[15] Thomas SA, Bye A, Segal MB. Transport characteristics of the anti-human immunodeficiency virus nucleoside analog, abacavir, into brain and cerebrospinal fluid. J Pharmacol Exp Ther 2001;298:947–53.
[16] Mahony WB, Domin BA, Daluge SM, Miller WH, Zimmerman TP. Enantiomeric selectivity of carbovir transport. J Biol Chem 1992;267:19792–7.
[17] Zimmerman TP, Wolberg G, Duncan GS. Inhibition of lymphocyte-mediated cytolysis by 3-deazaadenosine: evidence for a methylation reaction essential to cytolysis. Proc Natl Acad Sci USA 1978;75:6220–4.
[18] Domin BA, Mahony WB, Zimmerman TP. Purine nucleobase transport in human erythrocytes: reinvestigation with a novel ''inhibitor stop'' assay. J Biol Chem 1988;263:9276–84.
[19] Steck TL, Kant JA. Preparation of impermeable ghosts and inside-out vesicles from human erythrocyte membranes. In: Colowick SP, Kaplan NO, editors. Methods in enzymology, vol. XXXI. New York: Academic Press; 1974. p. 172–6.
[20] Daluge SM, Purifoy DJM. Savina PM, St. Clair MH, Parry NR, Dev IK, et al. 5-Chloro-2′,3′-dideoxy-3′-fluorouridine (935U83), a selective anti-human immunodeficiency virus agent with an improved metabolic and toxicological profile. Antimicrob Agents Chemother 1994;38:1590–603.
[21] Leatherbarrow RJ. Use of nonlinear regression to analyze enzyme kinetic data: application to situations of substrate contamination and background subtraction. Anal Biochem 1990;184:274–8.
[22] Cleland WW. Computer programmes for processing enzyme kinetic data. Nature 1963;198:463–5.
[23] Wilkinson GN. Statistical estimations in enzyme kinetics. Biochem J 1961;80:324–32.
[24] Cleland WW. The statistical analysis of enzyme kinetic data. Adv Enzymol 1967;29:1–32.
[25] Domin BA, Mahony WB, Zimmerman TP. Desciclovir permeation of the human erythrocyte membrane by nonfacilitated diffusion. Biochem Pharmacol 1991;42:147–52.
[26] Paterson ARP. Kolassa N, Cass CE. Transport of nucleoside drugs in animal cells. Pharmacol Ther 1981;12:515–36.
[27] Au JL, Su MH, Wientjes MG. Extraction of intracellular nucleosides and nucleotides with acetonitrile. Clin Chem 1989;35:48–51.
[28] Zimmerman TP, Domin BA, Mahony WB, Prus KL. Membrane transport of nucleoside analogues in mammalian cells. Nucleosides Nucleotides 1989;8:765–74.
[29] Belt JA, Marina NM, Phelps DA, Crawford CR. Nucleoside transport in normal and neoplastic cells. Adv Enzyme Regul 1993;33:235–52.
[30] Zimmerman TP, Mahony WB, Prus KL. 3′-Azido-3′-deoxythymidine, an unusual nucleoside analogue that permeates the membrane of human erythrocytes and lymphocytes by nonfacilitated diffusion. J Biol Chem 1987;262:5748–54.
[31] Painter GR, Shockcor JP, Andrews CW. Application of molecular mechanics to the study of drug-membrane interactions: the role of molecular conformation in the passive membrane permeability of zidovudine (AZT). In: Liotta D, editor. Advances in molecular modeling. Greenwich, CT: Jai Press; 1990. p. 135–63.
[32] Domin BA, Mahony WB, Koszalka GW, Porter DJT. Hajian G, Zimmerman TP. Membrane permeation characteristics of 5′-modified thymidine analogs. Mol Pharmacol 1992;41:950–6.
[33] Wright LL, Painter GR. Role of desolvation energy in the nonfacilitated membrane permeability of dideoxyribose analogs of thymidine. Mol Pharmacol 1992;41:957–62.
[34] Gati WP, Paterson ARP, Tyrrell DLJ, Cass CE, Moravek J, Robins MJ. Nucleobase transporter-mediated permeation of 2′,3′-dideoxyguanosine in human erythrocytes and human T-lymphoblastoid CCRF-CEM cells. J Biol Chem 1992;267:22272–6.
[35] Lanier ER, Sturge G, McClernon D, Brown S, Halman M, Sacktor N, et al. HIV-1 reverse transcriptase sequence in plasma and cerebrospinal fluid of patients with AIDS dementia complex treated with abacavir. AIDS 2001;15:747–51.
[36] Wilde MI, Langtry HD. Zidovudine: an update of its pharmacodynamic and pharmacokinetic properties, and therapeutic efficacy. Drugs 1993;46:515–78.